






Article

Palanquin-Like Cu_4Na_4 Silsesquioxane Synthesis (via Oxidation of 1,1-bis(Diphenylphosphino)methane), Structure and Catalytic Activity in Alkane or Alcohol Oxidation with Peroxides

Alena N. Kulakova ^{1,2}, Victor N. Khrustalev ^{2,3} , Yan V. Zubavichus ^{3,4} , Lidia S. Shul'pina ¹ , Elena S. Shubina ¹ , Mikhail M. Levitsky ¹, Nikolay S. Ikonnikov ¹, Alexey N. Bilyachenko ^{1,2,*}, Yuriy N. Kozlov ^{5,6} and Georgiy B. Shul'pin ^{2,5,6,*} 

¹ Nesmeyanov Institute of Organoelement Compounds, Russian Academy of Sciences, ul. Vavilova, 28, Moscow 119991, Russia; alenkulakova@gmail.com (A.N.K.); shulpina@ineos.ac.ru (L.S.S.); shu@ineos.ac.ru (E.S.S.); levitsk@ineos.ac.ru (M.M.L.); ikonns@ineos.ac.ru (N.S.I.)

² People's Friendship University of Russia, ul. Miklukho-Maklaya, dom 6, Moscow 117198, Russia; vnkhrustalev@gmail.com

³ National Research Center "Kurchatov Institute", pl. Akad. Kurchatova, dom 1, Moscow 123182, Russia; yzubav@googlegmail.com

⁴ Borekov Institute of Catalysis SB RAS, prosp. Akad. Lavrentieva, dom 5, Novosibirsk 630090, Russia

⁵ Semenov Institute of Chemical Physics, Russian Academy of Sciences, ul. Kosygina, dom 4, Moscow 119991, Russia; yunkoz@mail.ru

⁶ Chair of Chemistry and Physics, Plekhanov Russian University of Economics, Stremyannyi pereulok, dom 36, Moscow 117997, Russia

* Correspondence: bilyachenko@ineos.ac.ru (A.N.B.); gbsh@mail.ru or shulpin@chph.ras.ru (G.B.S.); Tel.: +7-499-135-9369 (A.N.B.); +7-495-939-7317 (G.B.S.)

Received: 26 December 2018; Accepted: 16 January 2019; Published: 4 February 2019



Abstract: The self-assembly synthesis of copper-sodium phenylsilsesquioxane in the presence of 1,1-bis(diphenylphosphino)methane (dppm) results in an unprecedented cage-like product: $[(\text{PhSiO}_{1.5})_6]_2[\text{CuO}]_4[\text{NaO}_{0.5}]_4[\text{dppmO}_2]_2$ **1**. The most intriguing feature of the complex **1** is the presence of two oxidized dppm species that act as additional O-ligands for sodium ions. Two cyclic phenylsiloxanolate $(\text{PhSiO}_{1.5})_6$ ligands coordinate in a sandwich manner with the copper(II)-containing layer of the cage. The structure of **1** was established by X-ray diffraction analysis. Complex **1** was shown to be a very good catalyst in the oxidation of alkanes and alcohols with hydrogen peroxide or *tert*-butyl hydroperoxide in acetonitrile solution. Thus, cyclohexane (CyH), was transformed into cyclohexyl hydroperoxide (CyOOH), which could be easily reduced by PPh_3 to afford stable cyclohexanol with a yield of 26% (turnover number (TON) = 240) based on the starting cyclohexane. 1-Phenylethanol was oxidized by *tert*-butyl hydroperoxide to give acetophenone in an almost quantitative yield. The selectivity parameters of the oxidation of normal and branched alkanes led to the conclusion that the peroxides H_2O_2 and *tert*-BuOOH, under the action of compound (**1**), decompose to generate the radicals HO^\bullet and *tert*-BuO $^\bullet$ which attack the C-H bonds of the substrate.

Keywords: alkanes; hydrogen peroxide; copper complexes; metallasilsesquioxanes; dppm oxidation

1. Introduction

Cage metallasilsesquioxanes (CLMSs) [1–10] are popular objects for the investigation of regularities in the insertion of metal ions into the siloxane matrix [11–18], the study of catalytic [19–24]

properties, magnetic (spin) glass [25], as well as the study of nanoparticles [26] and macrocyclic siloxane material [27] formation.

Among the synthetic approaches to cage metallasilsesquioxanes, the one based on the involvement of additional organic ligands has attracted significant attention due to the formation of extravagant molecular architectures, (e.g., [12,28–32]). In the continuation of these works, our team has recently suggested that the simplest method of the “mixed ligand synthesis” of CLMSs is to introduce additional organic ligand into the reaction mixture before the formation of the cage product. A modified self-assembly procedure such as this in most cases leads to the “ligand synergy” situation, with different ligands coordinating metal ions of the same cage compound. This feature was observed for several types on N-based ligands: 1,10-phenanthroline [33,34], 2,2'-bipyridine [33–35], and bathophenanthroline [34–36]. Dual behavior was detected for the neocuproine-assisted synthesis of Cu(II)-CLMS: in the case of DMF/dioxane reaction/crystallization media, a similar “ligand synergy product” was formed [37], while DMF media favors the isolation of “ligand antagonism” product with the redistribution of copper centers between silsesquioxane and neocuproine ligands [38], as seen in Figure 1. This particular antagonistic behavior was also found in the P-ligand-assisted self-assembly of Cu-CLMSs; this reaction was found to be tuned with two types of product being available for the reaction with 1,2-bis(diphenylphosphino)ethane [39], as seen in Figure 2.

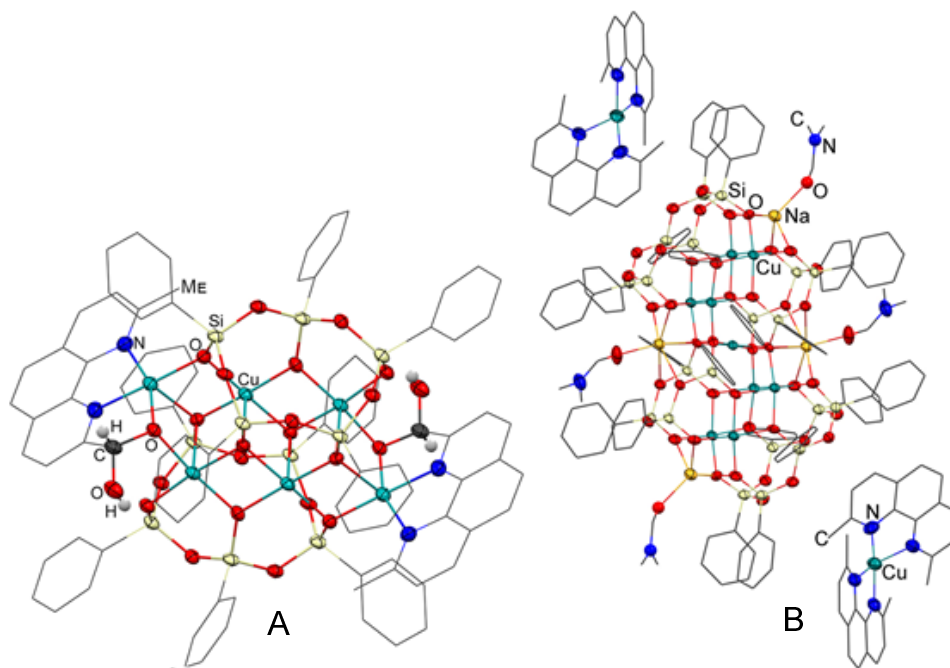


Figure 1. Features of cage Cu-CLMSs’ interaction with *N,N*-ligand (neocuproine). **Left:** Compound **A** with silsesquioxane and neocuproine ligands as parts of the same unit (Ref. [37]). **Right:** Ionic complex **B** with copper ions redistributed between silsesquioxane and neocuproine ligands (Ref. [38]). CLMS: cage metallasilsesquioxanes.

In the present article, we obtained non-trivial results from the synthesis with a close analogue of 1,2-bis(diphenylphosphino)ethane, namely, 1,1-bis(diphenylphosphino)methane (dppm). In the present article, we obtained non-trivial results from the synthesis with a close analogue of 1,2-bis(diphenylphosphino)ethane, namely, 1,1-bis(diphenylphosphino)methane (dppm). To our delight, the self-assembly reaction of $[(\text{PhSiO}_{1.5})(\text{NaO}_{0.5})]_n$ (obtained in situ from $\text{PhSi}(\text{OEt})_3$) with CuCl_2 in the presence of dppm resulted in the isolation (in a 22% yield) of heterometallic (Cu_4/Na_4) cage-like phenylsilsesquioxane **1**, as seen in Scheme 1.

The structure of **1** was established by an X-ray diffraction study, as seen in Figure 3 (see also ESI results). This study found that the formation of **1** was indeed accompanied by dppm ligands. Surprisingly, the way that dppm was found to act, is principally different to earlier mentions of dppe activity. Namely, dppm underwent in situ oxidation into its dioxide, dppmO₂, followed by the coordination to sodium ions. It is important to note that the oxidation of dppm to dppmO₂ was previously reported in the literature [40]. Moreover, some examples of oxidations during CLMS synthesis were described [33,34,37,41–45], but to the best of our knowledge, no single example of CLMS synthesis accompanied by dppm oxidation has been reported to date. An additional and intriguing feature of such oxidation that acted favorably in aiding the formation of **1** is the requirement of mild conditions. In this respect, we would like to suggest the influence of copper ions as catalytic centers and the presence of trace oxygen as an oxidant.

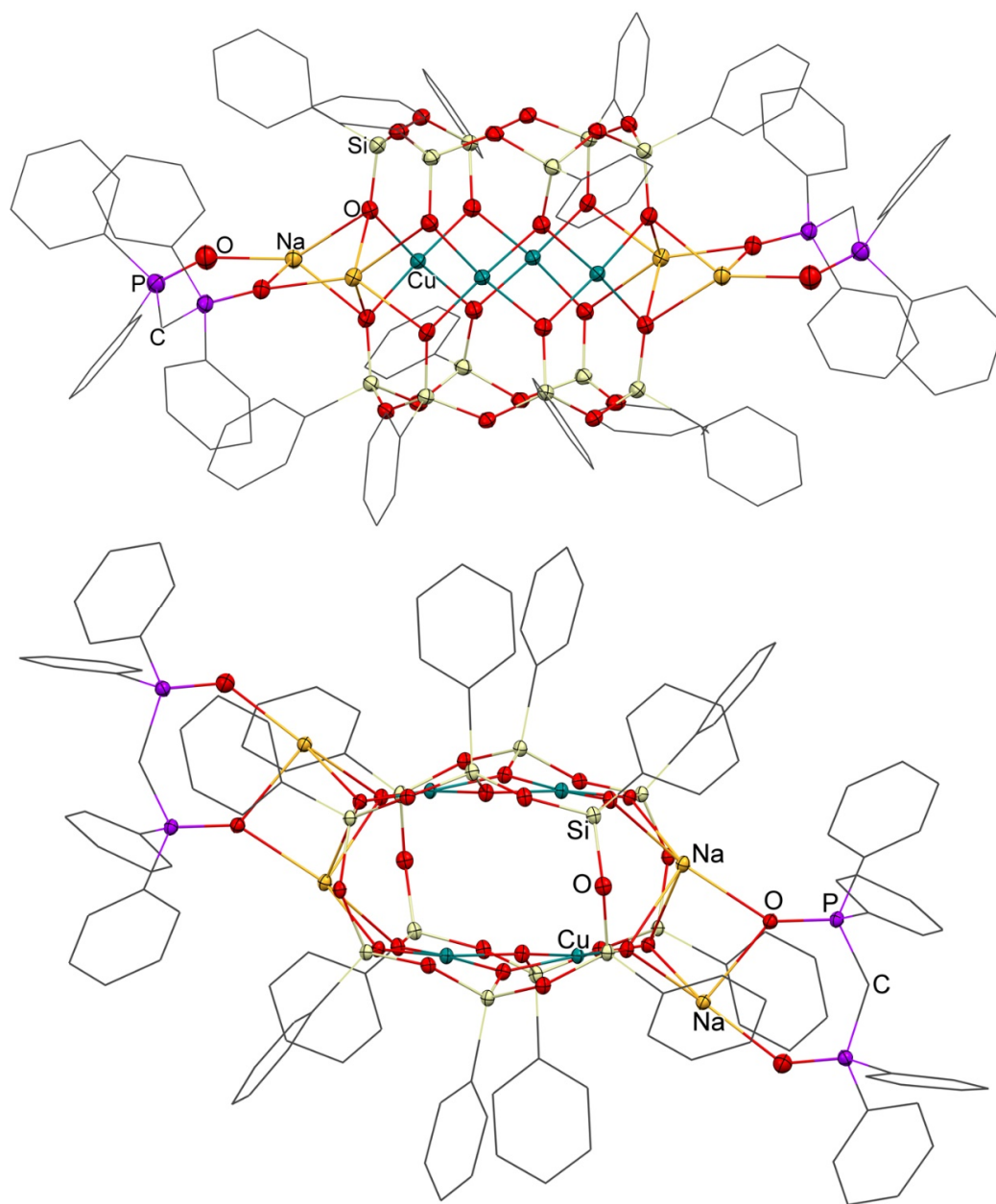


Figure 3. The molecular structure of **1**. **Top:** Front view. **Bottom:** Top view. Color code: copper—green, sodium—yellow, oxygen—red, phosphorous—purple.

Regarding the rest of the structure of **1**, it is also notable that the principle of cyclic silsesquioxane ligands' coordination to copper ions (in a sandwich manner as seen in Figure 4, left) is well-described in CLMSs chemistry [1,6,10]. In turn, the location of sodium ions in **1** is far from being classical. For a regular structure of sandwich CLMS, including four alkaline metal ions (e.g., Ref. [45]), it is quite easy to distinguish two pairs of alkaline metal ions (in axial and equatorial positions, respectively, as seen in Figure 4, center). In contrast to this, all of the sodium ions in **1** lay in equatorial positions, which allow for each dppmO₂ species to coordinate two sodium centers, as seen in Figure 4, right. Such coordination provokes a deep distortion of the sandwich skeletons of **1**, in comparison with similar fragments described in Refs. [39] (as seen in Figure 1) and [45] (as seen in Figure 2, center) (several distances and angles are provided in Table 1). The six-membered Na-dppm (Na-O-P-C-P-O) rings adopt a *sofa* conformation with the carbon atom out of the mean plane, which passed through the other atoms of the ring by 0.737(6) Å, as seen in Figure 3, A. The dihedral angle between the plane of Na,Cu-ions and the basal plane of the six-membered Na-dppm rings is 13.64(10)°: Additional crystallographic information is provided in the ESI (Tables S1–S6).

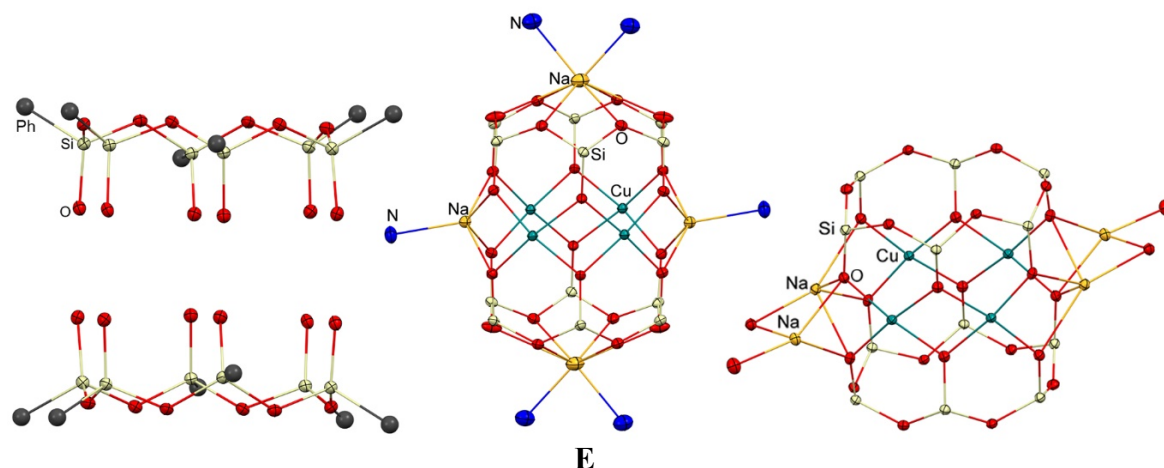


Figure 4. Left: Structure of silsesquioxane ligands in **1**. Center: Molecular structure of Cu₄-CLMSs from Ref. [45], representing the axial and equatorial locations of sodium centers. Right: The framework of **1**, representing equatorial-only locations of sodium centers. Color code: copper—green, sodium—yellow, oxygen—red, nitrogen—blue.

Table 1. Structural comparison of Cu₄-based CLMSs.

Compound	The Shortest Distance between Opposing Silicon Atoms in [PhSiO _{1.5}] ₆ Silsesquioxane Ligand, Å
1 (this work)	5.114
C (complex from Ref. [39])	5.584
E (complex from Ref. [45])	5.677

2. Oxidation of Hydrocarbons and Alcohols with Peroxides

Complexes of transition metals are known to catalyze the oxidation of hydrocarbons and alcohols with peroxides [46–50]. In the present work, we found that complex **1** exhibited catalytic activity in the oxidation of cyclohexane and other alkanes with H₂O₂ in acetonitrile, in the presence of nitric acid. Catalysts of this type have been shown to exhibit high catalytic activity. It was interesting to introduce phosphorus atoms into the catalyst structure.

The experiment shown in Figure 5 demonstrated that the reduction of the reaction solution with PPh₃ gave rise to a higher concentration of cyclohexanol and a decrease of cyclohexanone concentration (compare top and bottom graphs in Figure 5). These changes testify that the alkyl hydroperoxide was formed in the course of the oxidation (the so called Shul'pin method [51–64]).

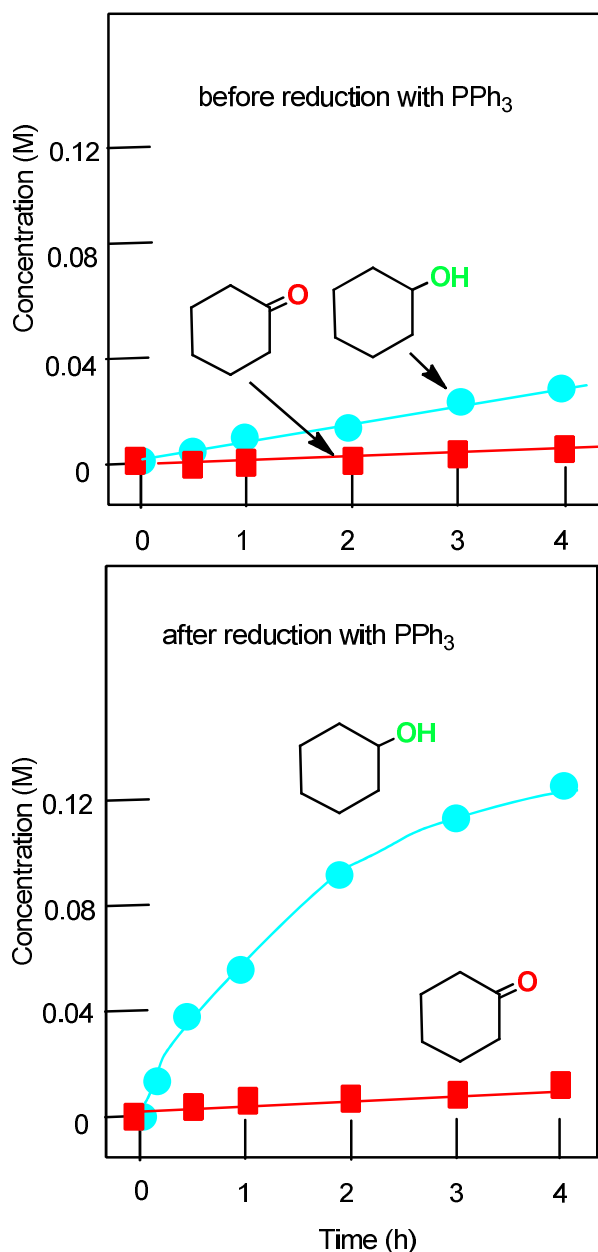


Figure 5. The accumulation of cyclohexanol and cyclohexanone in the oxidation of cyclohexane (0.46 M) with H₂O₂ (2 M) catalyzed by complex **1** (5×10^{-4} M), in the presence of HNO₃ (0.05 M) at 50 °C. In order to detect the formation of cyclohexyl hydroperoxide, the concentrations of the products were measured by GC before and after the reduction of the reaction sample with solid PPh₃. In the absence of HNO₃, the oxidation afforded only 0.015 M of products after 2 h (after the reduction of the reaction sample with solid PPh₃).

The following selectivity parameters were obtained for the oxidation of *n*-heptane: C(1):C(2):C(3):C(4) = 1.0:5.3:5.6:5.0 (after 1 h) and 1.0:6.1:5.8:5.8 (after 3 h); of methylcyclohexane: 1°:2°:3° = 1.0:5.4:15.0; and of *cis*-1,2-dimethylcyclohexane: *t/c* = 0.8 (the last parameter means that the *trans/cis* ratio of produced corresponding isomeric tertiary alcohols was 0.8). The character of dependence of the initial cyclohexane oxidation rate on the initial hydrocarbon concentration (approaching a plateau at [cyclohexane]₀ ~0.3 M; Figure 6), as well as the selectivity parameters measured here, indicate that the reaction occurred with the participation of hydroxyl radicals, and alkyl hydroperoxides were formed as the main primary products [65]. We assumed that added nitric acid induced the transformation of the catalyst into an active form.

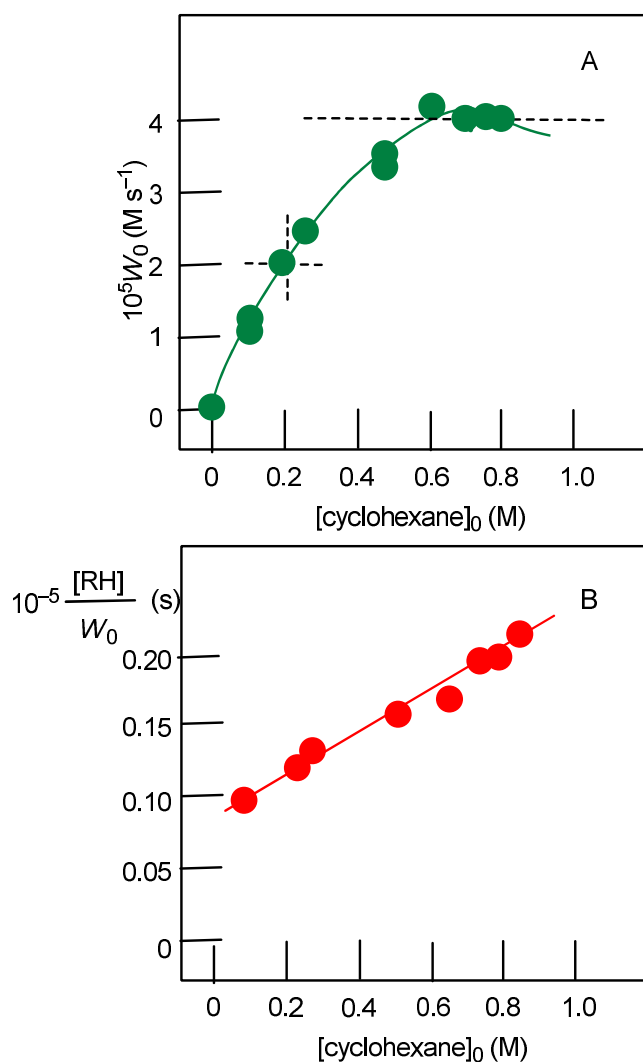


Figure 6. The dependence of the oxidation rate W_0 on the initial concentration of cyclohexane in the oxidation of cyclohexane into cyclohexanol and cyclohexanone (a sum) with H_2O_2 (2.0 M) catalyzed by complex **1** in the presence of HNO_3 (0.05 M). Conditions: catalyst **1** (5×10^{-4} M), 50°C , concentrations of products were measured by GC only after the reduction of the reaction sample with solid PPh_3 . Linearisation of the curve shown in Graph A is presented in Graph B.

The dependence of the reaction rate on the temperature of the reaction solution obeys the Arrhenius law, which allowed us to measure the effective activation energy (see Figure 7). The activation energy of cyclohexane oxidation was equal to 13.6 kcal/mol. The main increment of this value was from the process of catalytic H_2O_2 decomposition, which generated species inducing cyclohexane oxidation.

Complex **1** was found to efficiently catalyze the transformation of alcohols into the corresponding ketones by the oxidation with *tert*-butyl hydroperoxide, as seen in Figure 8.

The data presented in Figure 8 demonstrate that in the presence of complex **1** and *tert*-Bu-OOH, 1-phenylethanol was oxidized more effectively in comparison with cyclohexanol and heptanol-2. The characteristic times of the kinetic curves of the formation of corresponding ketones in the case that three alcohols were similar and that the maximum concentration of ketones including acetophenone was achieved when *tert*-Bu-OOH was completely diseased. Thus, the *tert*-Bu-OOH decomposition rates in the presence of three alcohols were similar and the active species generation rates for all alcohols were the same. The lower yields of ketones in comparison with the initial TBHP concentration were due to the concurrent reaction of TBHP with acetonitrile. 1-Phenylethanol exhibited a higher

reactivity in comparison with two other alcohols. This result was in accord with the known information regarding the higher constant that comes from the reaction of aromatic alcohols with hydroxyl radicals in comparison with constants measured for aliphatic alcohols [65].

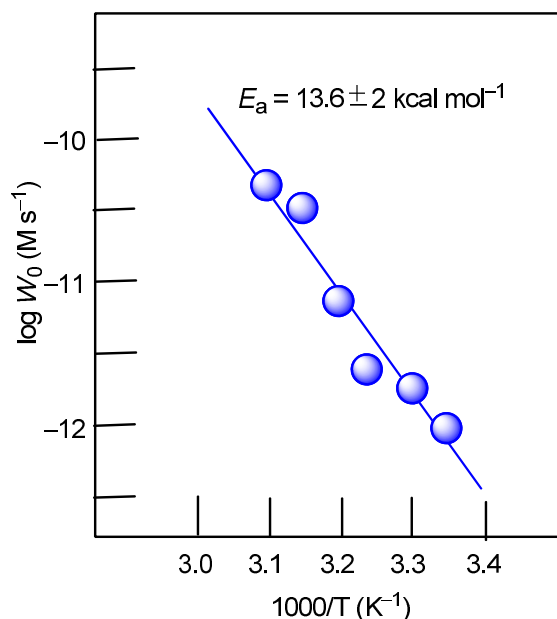


Figure 7. The Arrhenius plot of the oxidation of cyclohexane (0.46 M) with H_2O_2 (50%, 2 M), catalyzed by compound **1** (5×10^{-4} M) in acetonitrile, in the presence of HNO_3 (0.05 M). Concentrations of products were measured by GC after the reduction of the reaction sample with solid PPh_3 .

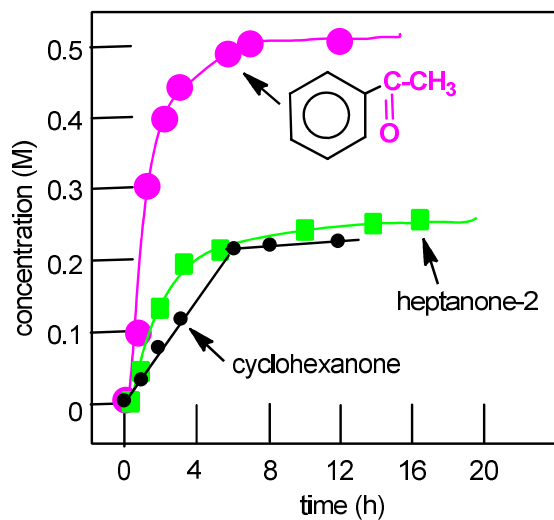
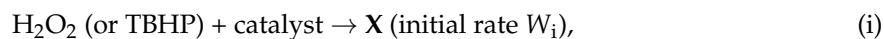


Figure 8. Accumulation of cyclohexanone, heptanone-2, and acetophenone in the oxidation of cyclohexanol (0.46 M), heptanol-2 (0.42 M), or 1-phenylethanol (0.5 M), respectively, with *tert*-butyl hydroperoxide (1.5 M) catalyzed by complex **1** (5×10^{-4} M) in the absence of HNO_3 at 50°C . In order to quench the oxidation process, concentrations of products were measured by GC only after the reduction of the reaction sample with solid PPh_3 .

The dependence of the initial 1-phenylethanol (ROH) oxidation rates by TBHP, as seen in Figure 9, on the initial ROH concentration was in accordance with an assumption on the oxidation of ROH by intermediate species generated in the catalytic peroxide decomposition. This species, **X**, reacts in two parallel routes with ROH and the solvent CH_3CN . Let us consider the following kinetic scheme:



Here, stage (i) reflects the process of the generation of X with the rate W_i ; stages (1) and (2) are from the processes of the interaction of X with ROH and CH_3CN , respectively, with the constants k_1 and k_2 . In the frames of quasi-stationary estimation, we can obtain the following equation for the initial rate of RO^\bullet generation:

$$(d[\text{R}_1\text{O}^\bullet]/dt)_0 = W_i / (1 + k_2[\text{CH}_3\text{CN}]/k_1[\text{ROH}]_0). \quad (3)$$

Analysis of the experimental data shown in Figures 6 and 9 in accordance with Equation (3) allowed us to determine the values of $k_2[\text{CH}_3\text{CN}]/k_1$ for the oxidation of ROH by hydrogen peroxide (0.44 M) and TBHP (0.33 M), respectively. These parameters were distinguished from the values typical for hydroxyl radicals (~ 0.1 M). However, the parameters of selectivity (see above) indicated that hydroxyl radicals took part in the oxidation with hydrogen peroxide. It is not yet clear what the reason for this discrepancy is, and this will be the subject of further research.

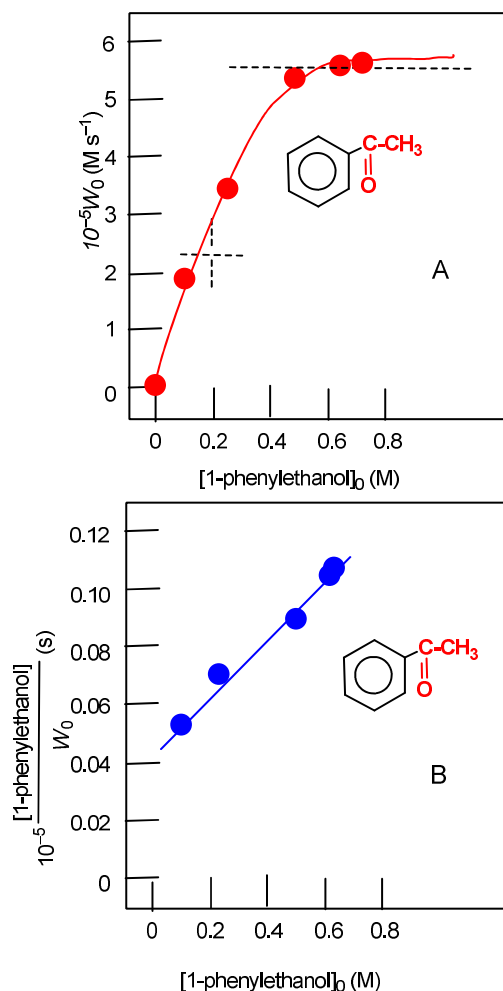


Figure 9. The dependence of the initial oxidation rate W_0 on the initial concentration of 1-phenylethanol in its oxidation into acetophenone with *tert*-butyl hydroperoxide (1.5 M) catalyzed by complex **1** (5×10^{-4} M), 50 °C. Concentrations of products were measured by GC only after the reduction of the reaction sample with solid PPh_3 in order to quench the oxidation process. Linearization of the curve, as shown in Graph A, is presented in Graph B.

3. Conclusions

The oxidation of 1,1-bis(diphenylphosphino)methane to its dioxide, under mild conditions, favored the formation of the unusual heterometallic cage silsesquioxane $[(\text{PhSiO}_{1.5})_6]_2[\text{CuO}]_4[\text{NaO}_{0.5}]_4[\text{dppmO}_2]_2$. The copper ions of the product were coordinated in a sandwich manner by two cyclic $(\text{PhSiO}_{1.5})_6$ ligands. In turn, sodium ions of the complex were located in the external positions and were ligated by both silsesquioxane species and dppmO_2 species. Such “oxidative activity” was additionally confirmed by catalytic tests. Cyclohexane, CyH , was transformed into cyclohexyl hydroperoxide CyOOH , which could be easily reduced by PPh_3 to afford stable cyclohexanol. 1-Phenylethanol was oxidized by *tert*-butyl hydroperoxide to give acetophenone in an almost quantitative yield. The selectivity parameters of oxidation of normal and branched alkanes led to the conclusion that peroxides H_2O_2 and *tert*-BuOOH under the action of compound **1** decomposed to generate the radicals HO^\bullet and *tert*-BuO $^\bullet$, which attacked the C-H bonds of the substrate.

Supplementary Materials: The following are available online at <http://www.mdpi.com/2073-4344/9/2/154/s1>, Table S1: Crystal data and structure refinement for **1**, Table S2: Atomic coordinates ($\times 10^4$) and equivalent isotropic displacement parameters ($\text{\AA}^2 \times 10^3$) for **1**. $U(\text{eq})$ is defined as one third of the trace of the orthogonalized U^{ij} tensor, Table S3: Bond lengths [\AA] and angles [$^\circ$] for **1**, Table S4: Anisotropic displacement parameters ($\text{\AA}^2 \times 10^3$) for **1**. The anisotropic displacement factor exponent takes the form: $-2\pi^2[h^2 a^{*2}U^{11} + \dots + 2hka^*b^*U^{12}]$, Table S5: Hydrogen coordinates ($\times 10^4$) and isotropic displacement parameters ($\text{\AA}^2 \times 10^3$) for **1**, Table S6: Torsion angles [$^\circ$] for **1**, Table S7: Hydrogen bonds for **1** [\AA and $^\circ$].

Author Contributions: A.N.B. and G.B.S. conceived and designed the experiments; A.N.K., Y.V.Z., V.N.K., N.S.I. and L.S.S. performed the experiments; A.N.B., E.S.S., M.M.L., Y.N.K. and G.B.S. analyzed the data; A.N.B. and G.B.S. wrote the paper.

Funding: This research was funded by the RUDN University Program “5-100”, the Russian Foundation for Basic Research (Grant Nos. 16-03-00254, 17-03-00993), the Ministry of Education and Science of the Russian Federation (project code RFMEFI61917X0007), as well as by the Initiative Program (State registration number AAAA-A16-116020350251-6) in the frames of the State Task 0082-2014-0007, “Fundamental regularities of heterogeneous and homogeneous catalysis”.

Acknowledgments: This work has been supported by the RUDN University Program “5-100”, the Russian Foundation for Basic Research (Grant Nos. 16-03-00254, 17-03-00993), the Ministry of Education and Science of the Russian Federation (project code RFMEFI61917X0007), as well as by the Initiative Program (State registration number AAAA-A16-116020350251-6) in the frames of the State Task 0082-2014-0007, “Fundamental regularities of heterogeneous and homogeneous catalysis”.

Conflicts of Interest: The authors declare no conflict of interest.

References

1. Murugavel, R.; Voigt, A.; Walawalkar, M.G.; Roesky, H.W. Hetero- and Metallasiloxanes Derived from Silanediols, Disilanol, Silanetriols, and Trisilanol. *Chem. Rev.* **1996**, *96*, 2205–2236. [[CrossRef](#)] [[PubMed](#)]
2. Lorenz, V.; Fischer, A.; Gießmann, S.; Gilje, J.W.; Gun’ko, Y.; Jacob, K.; Edelmann, F.T. Disiloxanediolates and polyhedral metallasilsesquioxanes of the early transition metals and f-elements. *Coord. Chem. Rev.* **2000**, *206–207*, 321–368. [[CrossRef](#)]
3. Hanssen, R.W.J.M.; van Santen, R.A.; Abbenhuis, H.C.L. The dynamic status quo of polyhedral silsesquioxane coordination chemistry. *Eur. J. Inorg. Chem.* **2004**, 675–683. [[CrossRef](#)]
4. Roesky, H.W.; Anantharaman, G.; Chandrasekhar, V.; Jancik, V.; Singh, S. Control of molecular topology and metal nuclearity in multimetallic assemblies: Designer metallasiloxanes derived from silanetriols. *Chem. Eur. J.* **2004**, *10*, 4106–4114. [[CrossRef](#)] [[PubMed](#)]
5. Lorenz, V.; Edelmann, F.T. Metallasilsesquioxanes. *Adv. Organomet. Chem.* **2005**, *53*, 101–153.
6. Levitsky, M.M.; Zavin, B.G.; Bilyachenko, A.N. Chemistry of metallasiloxanes. Current trends and new concepts. *Russ. Chem. Rev.* **2007**, *76*, 847–866. [[CrossRef](#)]
7. Jutzi, P.; Lindemann, H.M.; Nolte, J.O.; Schneider, M. Synthesis, Structure, and Reactivity of Novel Oligomeric Titanasiloxanes. In *Silicon Chemistry: From the Atom to Extended Systems*; Jutzi, P., Schubert, U., Eds.; Wiley: Hoboken, NJ, USA, 2007; pp. 372–382.

8. Edelman, F.T. Metallasilsesquioxanes. Synthetic and Structural Studies. In *Silicon Chemistry: From the Atom to Extended Systems*; Jutzi, P., Schubert, U., Eds.; Wiley: Hoboken, NJ, USA, 2007; pp. 383–394.
9. Ward, A.J.; Masters, A.F.; Maschmeyer, T. Metallasilsesquioxanes: Molecular Analogues of Heterogeneous Catalysts. *Adv. Silicon Sci.* **2011**, *3*, 135–166.
10. Levitsky, M.M.; Bilyachenko, A.N. Modern concepts and methods in the chemistry of polyhedral metallasiloxanes. *Coord. Chem. Rev.* **2016**, *306*, 235–269. [[CrossRef](#)]
11. Ovchinnikov, Y.E.; Zhdanov, A.A.; Levitsky, M.M.; Shklover, V.E.; Struchkov, Y.T. A cobaltoorganosiloxane with an unusual structure. *Bull. Acad. Sci. USSR Div. Chem. Sci.* **1986**, *35*, 1097. [[CrossRef](#)]
12. Feher, F.J. Polyhedral oligometallasilsesquioxanes (POMSS) as models for silica-supported transition-metal catalysts. Synthesis and characterization of (C₅Me₅)Zr[(Si₇O₁₂)(c-C₆H₁₁)₇]. *J. Am. Chem. Soc.* **1986**, *108*, 3850–3852. [[CrossRef](#)]
13. Winkhofer, N.; Voigt, A.; Dorn, H.; Roesky, H.W.; Steiner, A.; Stalke, D.; Reller, A. Stable Silanetriols as Building Blocks for the Synthesis of Titanasilsesquioxanes—Model Compounds for Titanium-Doped Zeolites. *Angew. Chem. Int. Ed. Engl.* **1994**, *33*, 1352. [[CrossRef](#)]
14. Zhdanov, A.A.; Sergienko, N.V.; Trankina, E.S. New method for the synthesis of cage and polymeric metallosiloxanes. *Russ. Chem. Bull.* **1998**, *47*, 2448–2450. [[CrossRef](#)]
15. Molodtsova, Y.A.; Pozdniakova, Y.A.; Lyssenko, K.A.; Blagodatskikh, I.V.; Katsoulis, D.E.; Shchegolikhina, O.I. A new approach to the synthesis of cage-like metallasiloxanes. *J. Organomet. Chem.* **1998**, *571*, 31–36. [[CrossRef](#)]
16. Hirotsu, M.; Taruno, S.; Yoshimura, T.; Ueno, K.; Unno, M.; Matsumoto, H. Synthesis and Structures of the First Titanium(IV) Complexes with Cyclic Tetrasiloxide Ligands: Incomplete and Complete Cage Titanosiloxanes. *Chem. Lett.* **2005**, *34*, 1542–1543. [[CrossRef](#)]
17. Zavina, B.G.; Sergienko, N.V.; Cherkun, N.V.; Bilyachenko, A.N.; Starikova, O.M.; Korlyukov, A.A.; Dronova, M.S.; Levitskii, M.M.; Timofeeva, G.I. Synthesis of Bimetallic Cage-Like Metalloorganosiloxanes From Polymeric Metallosiloxanes. *Russ. Chem. Bull.* **2011**, *60*, 1647–1650. [[CrossRef](#)]
18. Pinkert, D.; Demeshko, S.; Schax, F.; Braun, B.; Meyer, F.; Limberg, C. A Dinuclear Molecular Iron(II) Silicate with Two High-Spin Square-Planar FeO₄ Units. *Angew. Chem. Int. Ed.* **2013**, *52*, 5155–5158. [[CrossRef](#)] [[PubMed](#)]
19. Abbenhuis, H.C.L. Advances in Homogeneous and Heterogeneous Catalysis with Metal-Containing Silsesquioxanes. *Chem. Eur. J.* **2000**, *6*, 25–32. [[CrossRef](#)]
20. Duchateau, R. Incompletely Condensed Silsesquioxanes: Versatile Tools in Developing Silica-Supported Olefin Polymerization Catalysts. *Chem. Rev.* **2002**, *102*, 3525–3542. [[CrossRef](#)]
21. Levitsky, M.M.; Smirnov, V.V.; Zavina, B.G.; Bilyachenko, A.N.; Rabkina, A.Y. Metalasiloxanes: New structure formation methods and catalytic properties. *Kinet. Catal.* **2009**, *50*, 490–507. [[CrossRef](#)]
22. Quadrelli, E.A.; Basset, J.M. On silsesquioxanes' accuracy as molecular models for silica-grafted complexes in heterogeneous catalysis. *Coord. Chem. Rev.* **2010**, *254*, 707–728. [[CrossRef](#)]
23. Levitsky, M.M.; Yalymov, A.I.; Kulakova, A.N.; Petrov, A.A.; Bilyachenko, A.N. Cage-like metallasilsesquioxanes in catalysis: A review. *J. Mol. Catal. A Chem.* **2017**, *426 Pt B*, 297–304. [[CrossRef](#)]
24. Levitsky, M.M.; Bilyachenko, A.N.; Shul'pin, G.B. Oxidation of C-H compounds with peroxides catalyzed by polynuclear transition metal complexes in Si- or Ge-sesquioxane frameworks: A review. *J. Organomet. Chem.* **2017**, *849–850*, 201–218. [[CrossRef](#)]
25. Bilyachenko, A.N.; Yalymov, A.I.; Dronova, M.S.; Korlyukov, A.A.; Vologzhanina, A.V.; Es'kova, M.A.; Long, J.; Larionova, J.; Guari, Y.; Dorovatovskii, P.; et al. Family of Polynuclear Nickel Cagelike Phenylsilsesquioxanes; Features of Periodic Networks and Magnetic Properties. *Inorg. Chem.* **2017**, *56*, 12751–12763. [[CrossRef](#)] [[PubMed](#)]
26. Davies, G.L.; O'Brien, J.; Gun'ko, Y.K. Rare Earth Doped Silica Nanoparticles via Thermolysis of a Single Source Metallasilsesquioxane Precursor. *Sci. Rep.* **2017**, *7*, 45862. [[CrossRef](#)] [[PubMed](#)]
27. Yoshikawa, M.; Ikawa, H.; Wada, H.; Shimojima, A.; Kuroda, K. Self-assembly of cyclohexasiloxanes possessing alkoxysilyl groups and long alkyl chains. *Chem. Lett.* **2018**, *47*, 1203–1206. [[CrossRef](#)]
28. Fei, Z.; Busse, S.; Edelman, F.T. The first tantalasilsesquioxanes. *J. Chem. Soc. Dalton Trans.* **2002**, *12*, 2587–2589. [[CrossRef](#)]
29. Liu, F.; John, K.D.; Scott, B.L.; Baker, R.T.; Ott, K.C.; Tumas, W. Synthesis and Characterization of Iron Silsesquioxane Phosphane Complexes. *Angew. Chem. Int. Ed.* **2000**, *39*, 3127–3130. [[CrossRef](#)]

30. Nehete, U.N.; Anantharaman, G.; Chandrasekhar, V.; Murugavel, R.; Walawalkar, M.G.; Roesky, H.W.; Vidovic, D.; Magull, J.; Samwer, K.; Sass, B. Polyhedral Ferrous and Ferric Siloxanes. *Angew. Chem. Int. Ed.* **2004**, *43*, 3832–3835. [[CrossRef](#)]
31. Guillo, P.; Fasulo, M.E.; Lipschutz, M.I.; Tilley, T.D. Synthesis and characterization of tantalum silsesquioxane complexes. *Dalton Trans.* **2013**, *42*, 1991–1995. [[CrossRef](#)]
32. Tanabe, M.; Mutou, K.; Mintcheva, N.; Osakada, K. Preparation and NMR Studies of Palladium Complexes with a Silsesquioxanate Ligand. *Organometallics* **2008**, *27*, 519–523. [[CrossRef](#)]
33. Bilyachenko, A.N.; Kulakova, A.N.; Levitsky, M.M.; Petrov, A.A.; Korlyukov, A.A.; Shul'pina, L.S.; Khrustalev, V.N.; Dorovatovskii, P.V.; Vologzhanina, A.V.; Tsareva, U.S.; et al. Unusual Tri-, Hexa- and Nonanuclear Organosilicon Copper Clusters: Synthesis, Structures and Catalytic Activity in Oxidations with Peroxides. *Inorg. Chem.* **2017**, *56*, 4093–4103. [[CrossRef](#)] [[PubMed](#)]
34. Kulakova, A.N.; Bilyachenko, A.N.; Levitsky, M.M.; Khrustalev, V.N.; Korlyukov, A.A.; Zubavichus, Y.V.; Dorovatovskii, P.V.; Lamaty, F.; Bantreil, X.; Villemejeanne, B.; et al. Si₁₀Cu₆N₄ Cage Hexacoppersilsesquioxanes Containing N-Ligands: Synthesis, Structure, and High Catalytic Activity in Peroxide Oxidations. *Inorg. Chem.* **2017**, *56*, 15026–15040. [[CrossRef](#)] [[PubMed](#)]
35. Astakhov, G.S.; Bilyachenko, A.N.; Levitsky, M.M.; Korlyukov, A.A.; Zubavichus, Y.V.; Dorovatovskii, P.V.; Khrustalev, V.N.; Vologzhanina, A.V.; Shubina, E.S. Tridecanuclear Cu^{II}₁₁Na₂ Cagelike Silsesquioxanes. *Cryst. Growth Des.* **2018**, *18*, 5377–5384. [[CrossRef](#)]
36. Kulakova, A.N.; Bilyachenko, A.N.; Korlyukov, A.A.; Shul'pina, L.S.; Bantreil, X.; Lamaty, F.; Shubina, E.S.; Levitsky, M.M.; Ikonnikov, N.S.; Shul'pin, G.B. A new “bicycle helmet”-like copper(II),sodiumphenylsilsesquioxane. Synthesis, structure and catalytic activity. *Dalton Trans.* **2018**, *47*, 15666–15669. [[CrossRef](#)] [[PubMed](#)]
37. Bilyachenko, A.N.; Levitsky, M.M.; Khrustalev, V.N.; Zubavichus, Y.V.; Shul'pina, L.S.; Shubina, E.S.; Shul'pin, G.B. Mild and Regioselective Hydroxylation of Methyl Group in Neocuproine: Approach to an N,O-Ligated Cu₆ Cage Phenylsilsesquioxane. *Organometallics* **2018**, *37*, 168–171. [[CrossRef](#)]
38. Astakhov, G.S.; Bilyachenko, A.N.; Korlyukov, A.A.; Levitsky, M.M.; Shul'pina, L.S.; Bantreil, X.; Lamaty, F.; Vologzhanina, A.V.; Shubina, E.S.; Dorovatovskii, P.V.; et al. High-Cluster (Cu₉) Cage Silsesquioxanes: Synthesis, Structure, and Catalytic Activity. *Inorg. Chem.* **2018**, *57*, 11524–11529. [[CrossRef](#)] [[PubMed](#)]
39. Bilyachenko, A.N.; Kulakova, A.N.; Levitsky, M.M.; Korlyukov, A.A.; Khrustalev, V.N.; Vologzhanina, A.V.; Titov, A.A.; Dorovatovskii, P.V.; Shul'pina, L.S.; Lamaty, F.; et al. Ionic Complexes of Tetra- and Nonanuclear Cage Copper(II) Phenylsilsesquioxanes: Synthesis and High Activity in Oxidative Catalysis. *ChemCatChem* **2017**, *9*, 4437–4447. [[CrossRef](#)]
40. Berners-Price, S.J.; Norman, R.E.; Sadler, P.J. The autoxidation and proton dissociation constants of tertiary diphosphines: Relevance to biological activity. *J. Inorg. Biochem.* **1987**, *31*, 197–209. [[CrossRef](#)]
41. Gun'ko, Y.K.; Reilly, R.; Edelman, F.T.; Schmidt, H.G. The First Ce(IV) Metallasilsesquioxane Complex. *Angew. Chem. Int. Ed.* **2001**, *40*, 1279–1281. [[CrossRef](#)]
42. Gießmann, S.; Lorenz, V.; Liebing, P.; Hilfert, L.; Fischer, A.; Edelman, F.T. Synthesis and structural study of new metallasilsesquioxanes of potassium and uranium. *Dalton Trans.* **2017**, *46*, 2415–2419. [[CrossRef](#)]
43. Schax, F.; Bill, E.; Herwig, C.; Limberg, C. Dioxygen Activation by Siloxide Complexes of Chromium(II) and Chromium(IV). *Angew. Chem. Int. Ed.* **2014**, *53*, 12741–12745. [[CrossRef](#)] [[PubMed](#)]
44. Hay, M.T.; Hainaut, B.J.; Geib, S.J. Synthesis and characterization of a novel iron (III) silsesquioxane compound. *Inorg. Chem. Commun.* **2003**, *6*, 431–434. [[CrossRef](#)]
45. Kononevich, Y.N.; Anisimov, A.A.; Korlyukov, A.A.; Tsareva, U.; Shchegolikhina, O.I.; Muzafarov, A.M. Synthesis and structures of novel tetra- and pentanuclear copper sandwich-like metallasiloxanes with pyridine ligands. *Mendeleev Commun.* **2017**, *27*, 332–334. [[CrossRef](#)]
46. Wójtowicz-Młochowska, H. Synthetic utility of metal catalyzed hydrogen peroxide oxidation of C-H, C-C and C=C bonds in alkanes, arenes and alkenes: Recent advances. *Arkivoc* **2017**, *2017*, 12–58.
47. Shul'pin, G.B. Alkane-oxidizing systems based on metal complexes. Radical versus non-radical mechanisms. In *Alkane Functionalization*; Pombeiro, A.J.L., Ed.; Wiley: Hoboken, NJ, USA, 2018; Chapter 2.
48. Shul'pin, G.B. Metal-catalyzed oxidation of C-H compounds with peroxides in unconventional solvents. *Frontiers of Green Catalytic Selective Oxidations. Nat. Chem.* **2019**.
49. Shul'pin, G.B. New Trends in Oxidative Functionalization of Carbon–Hydrogen Bonds: A Review. *Catalysts* **2016**, *6*, 50. [[CrossRef](#)]

50. Shilov, A.E.; Shul'pin, G.B. *Activation and Catalytic Reactions of Saturated Hydrocarbons in the Presence of Metal Complexes*; Kluwer Academic Publishers: New York, NY, USA; Boston, MA, USA; Dordrecht, The Netherlands; London, UK; Moscow, Russia, 2002.
51. Shul'pin, G.B. Metal-catalysed hydrocarbon oxygenations in solutions: The dramatic role of additives: A review. *J. Mol. Catal. A Chem.* **2002**, *189*, 39–66. [[CrossRef](#)]
52. Shul'pin, G.B. Metal-catalysed hydrocarbon oxidations. *C. R. Chim.* **2003**, *6*, 163–178. [[CrossRef](#)]
53. Shul'pin, G.B.; Kozlov, Y.N.; Shul'pina, L.S.; Kudinov, A.R.; Mandelli, D. Extremely Efficient Alkane Oxidation by a New Catalytic Reagent $\text{H}_2\text{O}_2/\text{Os}_3(\text{CO})_{12}/\text{Pyridine}$. *Inorg. Chem.* **2009**, *48*, 10480–10482. [[CrossRef](#)]
54. Shul'pin, G.B.; Kozlov, Y.N.; Shul'pina, L.S.; Petrovskiy, P.V. Oxidation of alkanes and alcohols with hydrogen peroxide catalyzed by complex $\text{Os}_3(\text{CO})_{10}(\mu\text{-H})_2$. *Appl. Organometal. Chem.* **2010**, *24*, 464–472. [[CrossRef](#)]
55. Knops-Gerrits, P.P.; Trujillo, C.A.; Zhan, B.Z.; Li, X.Y.; Rouxhet, P.; Jacobs, P.A. Oxidation catalysis with well-characterised vanadyl bis-bipyridine complexes encapsulated in NaY zeolite. *Top. Catal.* **1996**, *3*, 437–449. [[CrossRef](#)]
56. Fornal, E.; Giannotti, C. Photocatalyzed oxidation of cyclohexane with heterogenized decatungstate. *Photochem. Photobiol. A Chem.* **2007**, *188*, 279–286. [[CrossRef](#)]
57. Shul'pin, G.B. Hydrocarbon Oxygenations with Peroxides Catalyzed by Metal Compounds. *Mini-Rev. Org. Chem.* **2009**, *6*, 95–104. [[CrossRef](#)]
58. Shul'pin, G.B. Selectivity enhancement in functionalization of C–H bonds: A review. *Org. Biomol. Chem.* **2010**, *8*, 4217–4228. [[CrossRef](#)] [[PubMed](#)]
59. Shul'pin, G.B. C–H Functionalization: Thoroughly tuning ligands at a metal ion, a chemist can greatly enhance catalyst's activity and selectivity. *Dalton Trans.* **2013**, *42*, 12794–12818. [[CrossRef](#)] [[PubMed](#)]
60. Maksimov, A.L.; Kardasheva, Y.S.; Predeina, V.V.; Kluev, M.V.; Ramazanov, D.N.; Talanova, M.Y.; Karakhanov, E.A. Iron and copper complexes with nitrogen-containing ligands as catalysts for cyclohexane oxidation with hydrogen peroxide under mild reaction conditions. *Petrol. Chem.* **2012**, *52*, 318–326. [[CrossRef](#)]
61. Shul'pin, G.B.; Druzhinina, A.N. Hydroperoxidation of alkanes by atmospheric oxygen in the presence of hydroquinone or quinone catalyzed by copper(II) acetate under visible light irradiation. *React. Kinet. Catal. Lett.* **1992**, *47*, 207–211. [[CrossRef](#)]
62. Shul'pin, G.B.; Nizova, G.V. Formation of alkyl peroxides in oxidation of alkanes by H_2O_2 catalyzed by transition metal complexes. *React. Kinet. Catal. Lett.* **1992**, *48*, 333–338. [[CrossRef](#)]
63. Garcia-Bosch, I.; Siegel, M.A. Copper-Catalyzed Oxidation of Alkanes with H_2O_2 under a Fenton-like Regime. *Angew. Chem. Int. Ed.* **2016**, *55*, 12873–12876. [[CrossRef](#)]
64. Olivo, G.; Lanzalunga, O.; Di Stefano, S. Non-Heme Imine-Based Iron Complexes as Catalysts for Oxidative Processes (Review). *Adv. Synth. Catal.* **2016**, *358*, 843–863. [[CrossRef](#)]
65. Buxton, G.V.; Greenstock, C.L.; Helman, W.P.; Ross, A.B. Rate constants for reactions of radicals in aqueous solution. *J. Phys. Chem. Ref. Data* **1988**, *17*, 513–886. [[CrossRef](#)]



© 2019 by the authors. Licensee MDPI, Basel, Switzerland. This article is an open access article distributed under the terms and conditions of the Creative Commons Attribution (CC BY) license (<http://creativecommons.org/licenses/by/4.0/>).